

# Isolated Dirac cone on the surface of ternary tetradymite-like topological insulators

H. Lin<sup>1</sup>, Tanmoy Das<sup>1,2</sup>, L. A. Wray<sup>3</sup>, S.-Y. Xu<sup>3</sup>, M. Z. Hasan<sup>3</sup>, and A. Bansil<sup>1</sup>

<sup>1</sup>*Department of Physics, Northeastern University,  
Boston, MA 02115, USA*

<sup>2</sup>*Theoretical Division, Los Alamos National Laboratory,  
Los Alamos, NM 87545, USA*

<sup>3</sup>*Joseph Henry Laboratories of Physics,  
Princeton University, Princeton,  
New Jersey 08544, USA*

We have extended our search for topological insulators to the ternary tetradymite-like compounds  $M_2X_2Y$  ( $M=\text{Bi}$  and  $\text{Sb}$ ;  $X$  and  $Y = \text{S}, \text{Se},$  and  $\text{Te}$ ), which are variations of the well-known binary compounds  $\text{Bi}_2\text{Se}_3$  and  $\text{Bi}_2\text{Te}_3$ . Our first-principles computations suggest that five existing compounds are strong topological insulators with a single Dirac cone on the surface. In particular, stoichiometric  $\text{Bi}_2\text{Se}_2\text{S}$ ,  $\text{Sb}_2\text{Te}_2\text{Se}$ , and  $\text{Sb}_2\text{Te}_2\text{S}$  are predicted to have an isolated Dirac cone on their naturally cleaved surface. This finding paves the way for realizing the topological transport regime.

Topological insulator is a very distinct state of quantum matter with a bulk-insulating gap of spin-orbit coupling (SOC) origin.<sup>1–11</sup> The Dirac fermions on the surface of a topological insulator possess topological quantum Berry phase and a definite spin chirality, which protects them from back-scattering and localization, resulting in counterpropagation of opposite spin states without dissipation. These are the key electronic ingredients for applications to topological quantum computing<sup>12,13</sup> and low-power spintronics<sup>14</sup> devices for which, however, the dissipationless surface states must be in the topological transport regime, i.e. to have an isolated Dirac cone fully separated from the bulk bands and the Fermi level to lie at the Dirac point.<sup>15</sup> The existing topological insulating materials fail in this regard due to their material-specific complications such as interference from numerous surface states<sup>16</sup>, shielding of the Dirac cone either inside the bulk-valence band<sup>17,18</sup> or the conduction bands<sup>19</sup>, or the involvement of crystal distortion in fabricating the material<sup>20,21</sup>.

Recently, it was shown experimentally that an isolated Dirac cone can be achieved by tuning the Fermi level with appropriate hole doping, but the non-stoichiometric crystal structure and the requirement of surface deposition generally makes this approach unsuitable for most practical applications.<sup>11,18</sup> On the other hand, solid solutions in the tetradymite-like compounds provide a platform for engineering topological surface states. For example, theoretical work of Zhang et al.<sup>22</sup> indicates the presence of a topological phase transition in  $\text{Sb}_2(\text{Te}_{1-x}\text{Se}_x)_3$  for  $0 \leq x \leq 1$ . Interestingly, since Se atoms preferentially occupy the central site in the crystal, at  $x=1/3$  the stoichiometric compound  $\text{Sb}_2\text{Te}_2\text{Se}$  can admit an ordered phase. Our recent work on topological insulator  $\text{Bi}_2\text{Te}_2\text{Se}$  reveals that the linewidth of the topological surface states in angle-resolved photoemission spectroscopy (ARPES) is narrow, indicating that disorder effects are suppressed in these compounds.<sup>23</sup> Ren et al.<sup>24</sup> have shown that  $\text{Bi}_2\text{Te}_2\text{Se}$  is the best material to date for

studying the topological surface states due to its highest bulk resistivity among all known topological insulators.

Here, we report first-principles computations on five existing tetradymite-like compounds  $\text{Bi}_2\text{Te}_2\text{Se}$ ,  $\text{Bi}_2\text{Te}_2\text{S}$ ,  $\text{Bi}_2\text{Se}_2\text{S}$ ,  $\text{Sb}_2\text{Te}_2\text{Se}$  and  $\text{Sb}_2\text{Te}_2\text{S}$  to show that these materials host salient topological insulating features in their stoichiometric crystal structures. Our important findings include that the last three of the five aforementioned compounds harbor an isolated Dirac cone with Dirac points which lie fully within the gap, allowing these states to reach the long-sought territory of the topological spin-transport regime<sup>6,15,25</sup> where the in-plane carrier transport would have a purely quantum topological origin.

Topological insulators in two- and three-dimensions have been predicted theoretically and observed experimentally as well to display quantum spin Hall effect<sup>3,4,26</sup> and strong topological behavior due to the combined effects of relativistic Dirac fermions and quantum entanglement<sup>1,3–11</sup>. For systems with inversion symmetry, a band inversion occurs due to a finite value of the spin-orbit coupling. This results in a bulk-insulating gap which ensures the existence of metallic surface states within the gap.<sup>16</sup> In bismuth or antimony metals, numerous surface states interfere with each other and an odd-number of Dirac cones can be achieved by making composite alloys such as  $\text{Bi}_{1-x}\text{Sb}_x$ .<sup>10</sup> In other novel classes of topological insulators, the Dirac node appears either below the valence band maximum as in  $\text{Bi}_2\text{Te}_3$  or  $\text{Sb}_2\text{Te}_3$ <sup>18</sup> or above the conduction band minimum as in  $\text{TlSbTe}_2$ .<sup>19</sup> Topologically nontrivial materials such as half-Heusler<sup>20</sup> and  $\text{Li}_2\text{AgSb}$ <sup>21</sup> series are semi-metals, which require lattice distortion to be tuned into the topological insulating state. For these reasons, it is difficult to electrically gate these materials for the manipulation and control of charge carriers for realizing a device. Therefore, a viable route to search for the isolated Dirac node in topological insulating materials is to find a chemically stable stoichiometric composition in an appropriate class of materials.

With this motivation, we consider in this article five ex-

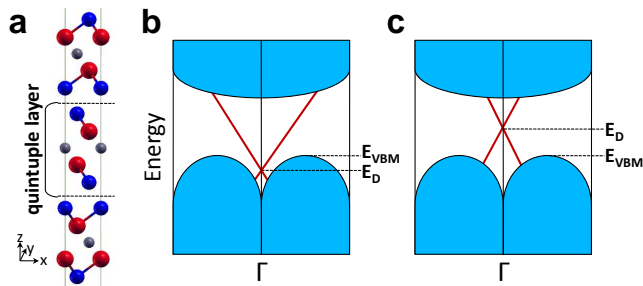


FIG. 1. **Tetradymite crystal structure and topological transport regime.** **a**, The crystal structure of tetradymite  $M_2X_2Y$ .  $M$ ,  $X$ , and  $Y$  atoms are denoted by red, blue, and grey balls, respectively. Diagrams in **b** and **c** illustrate surface band structures near the  $\Gamma$ -point for stoichiometric  $\text{Bi}_2\text{Te}_3$  and  $\text{Bi}_2\text{Se}_2\text{S}$ .

isting stoichiometric tetradymite-like ternary compounds in the structure  $M_2X_2Y$ , namely,  $\text{Bi}_2\text{Te}_2\text{Se}$ <sup>27</sup>,  $\text{Bi}_2\text{Te}_2\text{S}$ <sup>28</sup>,  $\text{Bi}_2\text{Se}_2\text{S}$ ,<sup>29</sup>  $\text{Sb}_2\text{Te}_2\text{Se}$ ,<sup>30</sup> and  $\text{Sb}_2\text{Te}_2\text{S}$ <sup>31</sup>. Tetradymite structure is with a rhombohedral unit cell of the space group  $R\bar{3}m$ . The commonly invoked hexagonal cell shown in Fig. 1a consists of three quintuple layers. The stacking order of two consecutive units may be represented as  $-X-M-Y-M-X--X-M-Y-M-X-$ . The layer of  $Y$  atoms is in the center of the unit. The natural surface termination is between the two  $X$ -atom layers. The known topological insulators  $\text{Bi}_2\text{Se}_3$ ,  $\text{Bi}_2\text{Te}_3$ , and  $\text{Sb}_2\text{Te}_3$  have the same crystal structure with  $X = Y$ .

Fig. 1b shows a schematic illustration of the bulk and surface band structures of  $\text{Bi}_2\text{Se}_3$ ,  $\text{Bi}_2\text{Te}_3$  and  $\text{Sb}_2\text{Te}_3$  in which the surface Dirac point lies below the valence band maximum (VBM). In our earlier experimental work, we lowered the Fermi level ( $E_F$ ) of  $\text{Bi}_2\text{Se}_3$  into the bulk bandgap by substituting trace amount of  $\text{Ca}^{2+}$  for  $\text{Bi}^{3+}$  with Ca acting as a hole donor to the bulk states. In order to lift the Dirac point above the VBM, we deposited  $\text{NO}_2$  on the surface. An isolated Dirac cone is then obtained as illustrated in Fig. 1c. In the present study, we predict new topological insulators  $\text{Bi}_2\text{Te}_2\text{Se}$ ,  $\text{Bi}_2\text{Te}_2\text{S}$ ,  $\text{Bi}_2\text{Se}_2\text{S}$ ,  $\text{Sb}_2\text{Te}_2\text{Se}$  and  $\text{Sb}_2\text{Te}_2\text{S}$ , among which the latter three have a Dirac point located in the bulk gap above the VBM as shown in Fig. 1c. Therefore, these three compounds are well-suited as materials with an isolated Dirac cone without requiring tuning via surface deposition. With proper electron/hole doping control or gating, one can position the  $E_F$  at the Dirac point and the material can be in the transport regime for potential device applications. We did not attempt to tune the electronic structure of the studied compounds using virtual crystal<sup>32,33</sup> or other first-principles approaches<sup>34,35</sup>.

The first-principles band structures were computed on the basis of experimental lattice data<sup>27-31</sup> within the framework of the density-functional theory (DFT) using the generalized-gradient approximation (GGA). Our results, shown in Fig. 2, predict that all these materials naturally host a topological insulating phase with band

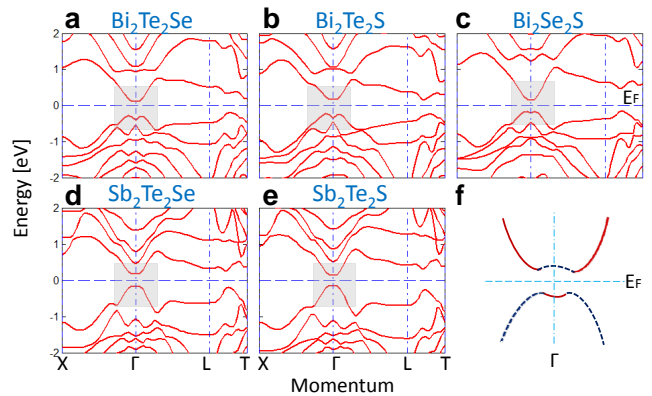


FIG. 2. **Bulk electronic structures and band-inversion.** Bulk electronic structures of  $\text{Bi}_2\text{Te}_2\text{Se}$  (**a**),  $\text{Bi}_2\text{Te}_2\text{S}$  (**b**),  $\text{Bi}_2\text{Se}_2\text{S}$  (**c**),  $\text{Sb}_2\text{Te}_2\text{Se}$  (**d**) and  $\text{Sb}_2\text{Te}_2\text{S}$  (**e**). The grey shaded areas in panels **a-e** highlight the inverted band structure as illustrated in panel **f**.

gaps in the range of 224 meV to 297 meV. A band inversion occurs at the  $\Gamma$ -point as highlighted with grey shadings. As illustrated in Fig. 2f, the conduction band (red solid line) and the valence band (blue dashed line) cross each other near the  $\Gamma$ -point, so that at this point the occupied state possess the character of the conduction band and the unoccupied state that of the valence band. Since the crystal has inversion symmetry, we have applied band parity analysis<sup>5</sup> to evaluate the value of the topological invariant  $Z_2$ . All five compounds are thus found to be strong topological insulators with  $Z_2 = -1$ . This comes about due to band inversion at the  $\Gamma$ -point through which the  $Z_2$  topological invariant picks up an extra factor of  $-1$  compared to bands without SOC. In short, the presence of an energy gap throughout the Brillouin zone with a band inversion only at the  $\Gamma$ -point makes this class of materials topological insulators.

The calculated DFT-GGA surface bands are shown in Fig. 3. A pair of surface bands with opposite spin directions are degenerate at the zone center and form the Dirac-cone-like dispersion. All five compounds exhibit a single Dirac cone inside the bulk band gap. For  $\text{Bi}_2\text{Te}_2\text{Se}$  and  $\text{Bi}_2\text{Te}_2\text{S}$ , the Dirac point lies below the VBM. This is the same as the case of stoichiometric binary  $\text{Bi}_2\text{Te}_3$  compound in which bulk scattering channels at the energy of the Dirac point prevent interesting quantum phenomena in the topological transport regime to be realized. The most interesting results are found in  $\text{Bi}_2\text{Se}_2\text{S}$ ,  $\text{Sb}_2\text{Te}_2\text{Se}$ , and  $\text{Sb}_2\text{Te}_2\text{S}$  where an isolated Dirac cone is obtained. Here, the Dirac point lies above the VBM and below the conduction bands. When  $E_F$  is tuned to the Dirac point, the density of states approaches zero and there are no other scattering channels. Therefore,  $\text{Bi}_2\text{Se}_2\text{S}$ ,  $\text{Sb}_2\text{Te}_2\text{Se}$ , and  $\text{Sb}_2\text{Te}_2\text{S}$  would be stoichiometric compounds which are well-suited for investigating the topological transport regime.

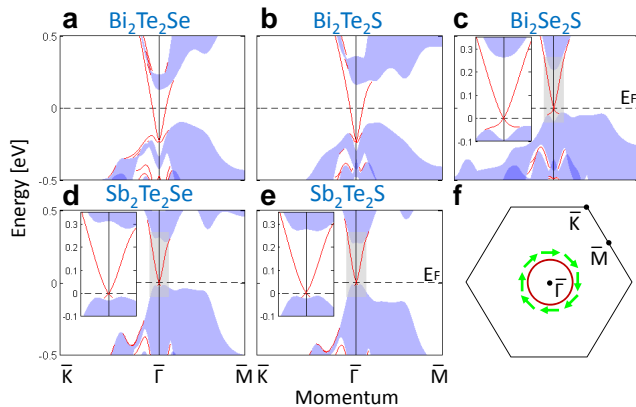


FIG. 3. **Surface states and spin-texture of the Dirac cone.** Surface band structures of  $\text{Bi}_2\text{Te}_2\text{Se}$  (a),  $\text{Bi}_2\text{Te}_2\text{S}$  (b),  $\text{Bi}_2\text{Se}_2\text{S}$  (c),  $\text{Sb}_2\text{Te}_2\text{Se}$  (d) and  $\text{Sb}_2\text{Te}_2\text{S}$  (e). Red lines are the surface states and the blue shaded areas are projected bulk states. Surface momentum is defined in panel f showing the hexagonal surface Brillouin zone. Green arrows in panel f denote the spin direction of the upper Dirac cone at constant energy (blue circle).

In conclusion, we predict that stoichiometric tetradymite-like compounds  $\text{Bi}_2\text{Te}_2\text{Se}$ ,  $\text{Bi}_2\text{Te}_2\text{S}$ ,  $\text{Bi}_2\text{Se}_2\text{S}$ ,  $\text{Sb}_2\text{Te}_2\text{Se}$ , and  $\text{Sb}_2\text{Te}_2\text{S}$  are strong topological insulators with large enough band gap for room temperature applications. The isolated Dirac cone on the surface of  $\text{Bi}_2\text{Se}_2\text{S}$ ,  $\text{Sb}_2\text{Te}_2\text{Se}$ , and  $\text{Sb}_2\text{Te}_2\text{S}$  will be particularly important for studying topological transport properties on a bulk material without the necessity of surface deposition.<sup>11</sup> Experiments with magnetic scattering techniques should be able to uniquely access the helical spin-texture of the isolated surface states which are

essential in device applications. The stoichiometric crystals of the investigated compounds are very easy to produce and manipulate for manufacturing devices for microchips,<sup>36</sup> spintronics<sup>14</sup> and information<sup>12,13</sup> technologies. Furthermore, the full exposure of the topological transport regime for dissipationless spin-current with the unique advantage of tunable surface states is suitable for studying novel topological phenomenon such as intrinsic quantum spin Hall effect,<sup>3,4,26</sup> universal topological magneto-electric effect<sup>37</sup> and anomalous half-integer quantization of Hall conductance<sup>6,38</sup>, and the quantum electrodynamical phenomena such as the image magnetic monopole induced by an electric charge<sup>39</sup> or Majorana fermions induced by the proximity effects from a superconductor<sup>12</sup>.

### Methods:

First-principles band calculations were performed with the linear augmented-plane-wave (LAPW) method using the WIEN2K package<sup>40</sup> within the framework of the density functional theory (DFT). The generalized gradient approximation (GGA) was used to describe the exchange-correlation potential.<sup>41</sup> Spin orbital coupling (SOC) was included as a second variational step using a basis of scalar relativistic eigenfunctions. The surface was simulated by placing a slab of 6 quintuple layers for  $\text{Bi}_2\text{Te}_2\text{Se}$  and  $\text{Bi}_2\text{Te}_2\text{S}$ . For  $\text{Bi}_2\text{Se}_2\text{S}$ ,  $\text{Sb}_2\text{Te}_2\text{Se}$  and  $\text{Sb}_2\text{Te}_2\text{S}$  we used 12 quintuple layers to ensure convergence with the number of layers.

**Acknowledgements:** The work at Northeastern and Princeton is supported by the Division of Materials Science and Engineering, Basic Energy Sciences, US Department of Energy (DE-FG02-07ER46352, DE-FG-02-05ER46200 and AC03-76SF00098), and benefited from the allocation of supercomputer time at NERSC and Northeastern University's Advanced Scientific Computation Center (ASCC). Support from the A. P. Sloan Foundation (L.A.W., S.Y.X, and M.Z.H.) is acknowledged.

- 
- <sup>1</sup> For a brief review see, Moore, J. E., *Nature* **464**, 194-198 (2010).  
<sup>2</sup> Hasan, M. Z., and Kane, C. L., *Rev. Mod. Phys.* **82**, 3045 (2010).  
<sup>3</sup> Kane, C. L., & Mele, E. J., *Phys. Rev. Lett.* **95**, 146802 (2005).  
<sup>4</sup> Bernevig, B. A., Hughes, T. L., Zhang, S.-C., quantum wells. *Science* **314**, 1757-1761 (2006).  
<sup>5</sup> Fu, L. & Kane, C. L., *Phys. Rev. B* **76**, 045302 (2007).  
<sup>6</sup> Fu, L., Kane, C. L., & Mele, E. J., *Phys. Rev. Lett.* **98**, 106803 (2007).  
<sup>7</sup> Moore, J. E. & Balents, L., *Phys. Rev. B* **75**, 121306(R) (2007).  
<sup>8</sup> Roy, R., *Phys. Rev. B* **79**, 195322 (2009).  
<sup>9</sup> König, M. et al., *Science* **318**, 766-770 (2007).  
<sup>10</sup> Hsieh, D. et al., *Nature* **452**, 970-974 (2008).  
<sup>11</sup> Hsieh, D. et al., *Nature* **460**, 1101-1105 (2009).  
<sup>12</sup> Fu, L. & Kane, C. L., surface of a topological insulator, *Phys. Rev. Lett.* **100**, 096407 (2008).  
<sup>13</sup> Leek, P.J. et al., *Science* **318** 1889-1892 (2007).  
<sup>14</sup> Wolf, S. A. et al., *Science* **294** 1488-1495 (2001).  
<sup>15</sup> Fu, L. & Kane, C. L., *Phys. Rev. Lett.* **102**, 216403 (2009).  
<sup>16</sup> Zhang, H. et al., *Nature Phys.* **5**, 438-442 (2009).  
<sup>17</sup> Xia, Y. et al., *Nature Phys.* **5**, 398-402 (2009).  
<sup>18</sup> Hsieh, D. et al., *Phys. Rev. Lett.* **103**, 146401 (2009).  
<sup>19</sup> Lin, H. et al., *Phys. Rev. Lett.* **105**, 036404 (2010).  
<sup>20</sup> Lin, H. et al., *Nature Mat.* **9**, 546 (2010).  
<sup>21</sup> Lin, H. et al., Preprint at <http://arxiv.org/abs/1004.0999> (2010).  
<sup>22</sup> Zhang, W. et al., *New Journal of Physics* **12**, 065013 (2010).  
<sup>23</sup> Xu, S.-Y. et al., Preprint at <http://arxiv.org/abs/1007.5111v1> (2010).  
<sup>24</sup> Ren, Z. et al., *Phys. Rev. B* **82**, 241306(R) (2010).  
<sup>25</sup> Qi, X.-L., Hughes, T. L. & Zhang, S.-C., *Phys. Rev. B* **78**, 195424 (2008).  
<sup>26</sup> Bernevig B. A., & Zhang S.-C. *Phys. Rev. Lett.* **98**, 106802 (2006).

- <sup>27</sup> Mishra, S. & Bever, M. B., *J. Phys. Chem. Solids* **25** 1233-1241 (1964).
- <sup>28</sup> Harker, D., *Z. Kristallographie* **89** 175-181 (1934).
- <sup>29</sup> ChiChagov, A.V. *et al.*, (MINCRYST). *Kristallographya* **35** 610-616 (1990).
- <sup>30</sup> Anderson, T. L. & Krause, H. B., their relationship *Acta Cryst.* **B30** 1307 (1974).
- <sup>31</sup> Grauer, D. C., Hor, Y.S., Williams A. J. & Cava, R. J., *Mat. Res. Bulletin* **44** 1926-1929 (2009).
- <sup>32</sup> Bansil, A., *Zeitschrift Naturforschung A: Phys. Sci.* **48** 165 (1993). **48**, 165 (1993).
- <sup>33</sup> Lin, H., Sahrakorpi, S., Markiewicz, R. S., and Bansil, A., *Phys. Rev. Lett.* **96** 097001 (2006) Bi<sub>2</sub>Sr<sub>2</sub>CaCu<sub>2</sub>O<sub>8</sub>+?? and Other Cuprate *Phys. Rev. Lett.* **96**, 097001 (2006).
- <sup>34</sup> Bansil, A., Kaprzyk, S., Mijnaerends, P. E., and Tobola, J., *Phys. Rev. B* **60** 13396 (1999); Mijnaerends, P. E., and Bansil, A., *Phys. Rev. B* **13** 2381-2390 (1976). alloys by the KKR-CPA method *Phys. Rev. B* **13**, 2381 (1976).
- <sup>35</sup> Khanna, S. N., Ibrahim, A. K., McKnight, S. W., and Bansil, A., *Solid State Commun.* **55** 223-226 (1985); Huisman, L., Nicholson, D., Schwartz, L., and Bansil, A., *Phys. Rev. B* **24** 1824-1834 (1981). disordered metals: Application to liquid Cu Bansil, *Solid State*
- <sup>36</sup> Seradjeh, B., Moore, J.E., & Franz, M., insulator film. Preprint at (<http://arxiv.org/abs/0902.1147>) (2009).
- <sup>37</sup> Essin, A. Moore, J. E. & Vanderbilt, D., *Phys. Rev. Lett.* **102** 146805 (2009).
- <sup>38</sup> Qi, X.-L., Hughes, T. L. & Zhang, S.-C., *Phys. Rev. B* **78**, 195424 (2008).
- <sup>39</sup> Qi, X.-L, Li, R., Zhang, J. & Zhang, S.-C., *Science* **323** 1184 (2009).
- <sup>40</sup> Blaha, P., Schwarz, K., Madsen, G. K. H., Kvasnicka, D. & Luitz, J. *WIEN2k, An Augmented Plane Wave Plus Local Orbitals Program for Calculating Crystal Properties.* (Karlheinz Schwarz, Techn. University Wien, Austria, 2001).
- <sup>41</sup> Perdew, J. P., Burke, K. & Ernzerhof, M., *Phys. Rev. Lett.* **77**, 3865-3868 (1996).